ELSEVIER

Chemical Engineering Journal 86 (2002) 173–178

Chemical Engineering Journal

www.elsevier.com/locate/cej

Modeling of moisture profiles in paddy rice during drying mapped with magnetic resonance imaging

J.M. Frías [a], L. Foucat [b], J.J. Bimbenet [a], C. Bonazzi [a,*]

[a] *JRU of Food Process Engineering, Cemagref-ENSIA-INAPG-INRA, 1 Avenue des Olympiades, 91744 Massy Cedex, France*

[b] *INRA, SRV-STIM, 63122 St. Genes Champanelle, France*

Abstract

During the drying process, internal water migration is often the limiting factor for the overall water transfer. In order to simulate a drying process, an accurate determination of the water diffusivity ($\mathcal{D}$) in the material is always necessary. For biological products $\mathcal{D}$ is known to be low and vary with moisture content (X) and temperature (T). $\mathcal{D} = f(X, T)$ can be estimated from the fitting of moisture profiles determined by non-intrusive NMR imaging. This work first presents the experimental results obtained on paddy rice. The moisture profiles were measured during the drying process using a Bruker AMX400 spectrometer, equipped with a micro-imaging device at the H^+ frequency of 400 MHz. Four drying experiments at two different air temperatures were performed. A constant time imaging (CTI) technique proved to be useful to obtain the moisture content map in a central slice section of the kernel with 3 mm thickness, allowing a spatial resolution of 0.1 mm. This method provided access to low moisture content and low water mobility data. Then a diffusive model was developed using a cylindrical geometry, taking into consideration the shrinkage during drying. Uni-dimensional water profiles from axes of the elliptic section of the kernel were selected in order to determine the diffusivity parameters of the drying model. © 2002 Elsevier Science B.V. All rights reserved.

Keywords: NMR; Diffusivity; Moisture transport phenomena; Parameter estimation

1. Introduction

The water transport phenomena in paddy rice and in any other cereal that has to be dried after harvesting is an essential process for both final quality of the product and economic benefit of the producer. Contrary to other cereals, rice is preferably consumed as whole grains; therefore an important criterion for the rice industry is the head rice yield after milling, which is the percentage of non-broken kernels after removal of hulls and bran of the rough rice grain on a mill. Drying, harvesting and storage induce cracks in the grain leading to breakage during processing. Mechanical damage in rice is closely related with the severity of the drying process and especially with the increase of the moisture gradients inside the grain. It is due to the fact that mechanical properties of a food material vary significantly with moisture content and temperature and that drying induces non-uniform deformations responsible for stress and stain in the kernel. MRI is a technique that has been successfully used for non-intrusive measurement of moisture distribution in solids during drying. MRI studies of water distribution during drying of a pulp sheet have achieved resolutions that are in the order of magnitude needed for a rice kernel [1]. Kovács and Neményi [2] studied the moisture gradient history during the drying of maize kernels. Fukuoka et al. [3] and Takeuchi et al. [4,5] studied the moisture profiles in rice grains during the cooking process and compared the results with a diffusive model. McCarthy and Perez [6], Ruiz-Cabrera et al. [7] and Hills et al. [8] used the Boltzmann transformation of MRI uni-dimensional profile data to determine the water diffusivity in apple or gelatin. Verstreken et al. [9] determined parameters of a diffusive model from NMR profile data on apples. Despite the advantage of being a very precise nondestructive analytical technique, MRI presents some inherent difficulties, like a complex calibration and data handling work, errors in the determination of the physical boundaries and possible low signal to noise ratios. Those issues have to be considered in order to arrive to a correct understanding of the collected data [10].

The objective of this work is to perform non-intrusive measurement of moisture profiles in a paddy rice kernel during drying using MRI techniques and to use the generated data in order to obtain a mathematical model and diffusivity parameters that can characterize the moisture transport during drying.

* Corresponding author. Tel.: +33-1-6993-5026; fax: +33-1-6993-5185.
E-mail address: bonazzi@ensia.inra.fr (C. Bonazzi).

1385-8947/02/$ – see front matter © 2002 Elsevier Science B.V. All rights reserved.
PII: S1385-8947(01)00285-6

Nomenclature

a	pre-exponential factor (g dry matter/g water)
c_p	specific heat (J/kg K)
$\mathcal{D}$	diffusivity (m^2/s)
E_a	activation energy (kJ/mol K)
k_p	external mass transfer coefficient (kg/m^2 Pa s)
P_v	vapor pressure (Pa)
r	eulerian dimension (m)
R	radius of the equivalent cylinder (m)
R^2_{adj}	determination coefficient adjusted to the degrees of freedom (–)
S	MRI signal (–)
S_v	surface volume ratio (m^{-1})
t	time (s)
t_{pw}	encoding time (ms)
t_r	repetition time (ms)
T	temperature (°C)
T_1	spin–lattice relaxation time (ms)
T_2	spin–spin relaxation time (ms)
T_{db}	dry bulb temperature (°C)
X	moisture content (kg water/kg dry matter)

Greek letters

β	shrinkage coefficient (g dry matter/g water)
θ	flip angle (°)
λ_m	thermal conductivity (W/m K)
λ_v	heat of evaporation (J/kg)
ξ	lagrangian dimension (m dry matter)
ρ_s	solid density (kg/m^3)
σ_{res}	residuals standard deviation

Subscripts

0	initial
$*$	dry
m	external boundary
ref	reference
s	solids

2. Materials and methods

2.1. Product

Long grains rough rice of the Ariete variety were used for all tests, from samples harvested to about 25% d.b. in Camargue, France. Paddy rice samples were conditioned at 10 different moisture contents at 25 °C using the methodology from [11].

2.2. MRI experiments

The NMR apparatus was a Bruker AMX 400 with a 9.4 T magnet (H^+ resonance frequency of 400 MHz) equipped with micro-imaging instrumentation.

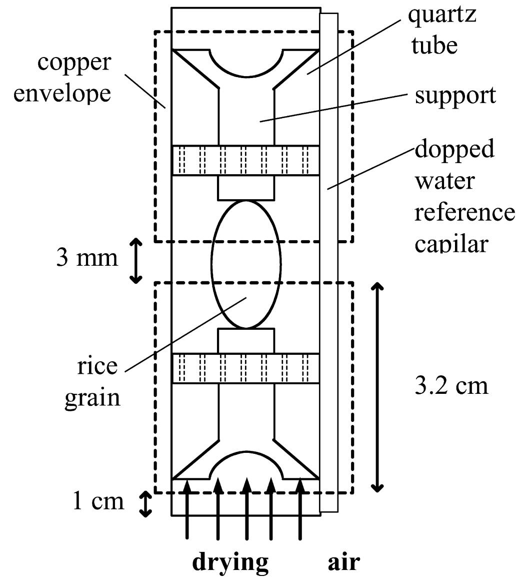

Fig. 1. Sample carrier for the MRI drying experiments.

First, classical spectrometric measurements (CPMG and inversion recovery sequences) were performed in order to determine T_1 and T_2 dependence on moisture content. These measurements were performed on rice grain cylinders, where the top and the bottom of the grain were cut. This procedure was performed with paddy and white rice, equilibrated at six different moisture contents (from 0.03 to 0.19 g water/g dry matter) and at two different sample temperatures (30 and 60 °C).

In order to perform the imaging experiments, a sample carrier that maintained the rice grain in the center of the coil during drying was designed (Fig. 1). A physical barrier (copper envelope) to the radio frequency was added, in order to collect the signal from only a 3 mm height central section of the rice grain. In this section, the kernel is considered as a perfect cylinder and the influence of the composition of the embryo on signal is hidden. Finally, a doped water capillary was placed next to the quartz tube in order to determine the proportionality coefficient of the MRI signal with water content. MRI experiments were developed with the use of a constant time imaging (CTI) sequence.

Such CTI sequences have been used recently to follow the moisture migration in samples with low moisture content, where faster image acquisition times than those obtained with spin-echo images are required [12,13]. CTI sequences were performed using a two-dimensional magnetic field gradient in the transversal direction of the rice grain (x and y directions in the NMR coil, integrating the whole height of the observed central slice of the rice grain). The sequence used a repetition time of $t_r = 50$ ms, a flip angle $\theta = 16°$ and an encoding time of $t_{pw} = 150$ ms, which maximized the contrast of the water protons in the rice kernel (the 'water' image). At the beginning of the experiment, another image (the 'fat' image) with a $t_{pnw} = 1000$ ms maximizing the contrast of the non-water protons of the rice kernel was taken. The total image acquisition time was 13 min and 41 s, which is a reasonable time for data acquisition if compared with the total drying times (over 6 h).

Four drying experiments were performed using rice grains equilibrated to an initial moisture content of 0.19 kg water/kg dry matter. Two of them were performed with air drying at 30 °C (with relative humidities of 30 and 27%, respectively) and the other two at 60 °C (with relative humidities of 7 and 6%, respectively), with an averaged air speed of 0.9 m/s.

2.3. Numerical methods

All the treatment of the NMR data spectra was performed using the Xstim software (STIM-SRV, INRA-Theix, France). The transformation of the profiles to moisture content was performed with Scilab (INRIA, France) and the mathematical modeling of the moisture profile was performed using Fortran77 (using ODRPACK library for the parameter estimation from [14] and ODEPACK from [15] for the numerical simulation).

3. Results and discussion

3.1. Spectrometric experiments

Only two peaks contributed to the Fourier transformed spectra signal. The first one was identified as the signal coming from water protons by comparing spectra from kernels at different water contents; these spectra showed a decrease in the peak height correlated with the decrease in water content. The second one was identified as the signal from the non-water protons, mainly lipids from the external aleurone layer, by analyzing spectra of paddy and polished white rice. This conclusion was deduced from the fact that spectra of white rice samples (obtained after removal of most of the bran protein and oil) did not present any second peak.

The relaxation times T_1 and T_2 for the water and non-water peaks together with their respective standard errors were determined at six different moisture contents and two different temperatures (30 and 60 °C) from a parametric estimation using a nonlinear time series model. Then, an inverse weighted linear regression with the T_1 data was performed (using the inverse of the previously obtained T_1 standard errors as weights in the regression) to obtain the dependence of T_1 on moisture and temperature for the water proton peak:

$$T_{1_{\mathrm{w}}} = \frac{10^3}{42.3X + 0.014X - 0.11XT - 4.1} \quad (R^2_{\mathrm{adj}} = 0.92) \tag{1}$$

and for the non-water proton peak:

$$T_{1_{\mathrm{nw}}} = \frac{10^3}{20.2X + 0.011T - 0.053XT - 4.8} \quad (R^2_{\mathrm{adj}} = 0.98) \tag{2}$$

The spin–spin relaxation times for the same peaks were considered constant with average values of $T^*_{2_{\mathrm{w}}} = 279\ \mu\mathrm{s}$ and $T^*_{2_{\mathrm{nw}}} = 531\ \mu\mathrm{s}$.

3.2. Transformation of the MRI signal to water content

The obtained signal was a mixture of water and non-water proton contributions, due to the characteristics of both the MRI sequence and the relaxation times of the two spectra peaks. The qualitative analysis of the 'fat' image showed that the lipid contribution to the proton signal was low and concentrated mainly in an annular section of the image, which presented too much noise to perform a quantitative procedure. Assuming that the non-water proton contribution was negligible, the water concentration in dry basis for each pixel of the image was finally calculated using Eq. (3) from [16]

$$S_{\mathrm{rice}} = k \frac{\rho^*_{\mathrm{s}} X}{1 + \beta X} \frac{1 - \mathrm{e}^{-t_r/T_{1_{\mathrm{w}}}(X,T)}}{1 - \cos(\theta)\, \mathrm{e}^{-t_{\mathrm{r}}/T_{1_{\mathrm{w}}}(X,T)}} \sin(\theta)\, \mathrm{e}^{-t_{p_{\mathrm{w}}}/T^*_2} \tag{3}$$

The k coefficient of proportionality was calculated from the averaged signal of the central section of the doped water capillary tube, where the volumetric water concentration was known. This moisture transformation procedure was validated by calculating the average moisture content using data of the images taken at the initial times and comparing it to the measured values (∼0.19 kg water/kg dry matter), with a satisfactory agreement between the initial profile and the gravimetric data. Examples of the evolution and moisture profiles of the water images during a drying process can be seen in Figs. 2 and 3, showing the sensitivity of the MRI technique to the drying kinetics.

The non-uniform initial moisture content profile of the paddy can be observed, with a higher concentration of water at the center of the grain. These data also show that it was possible to observe the evolution of the moisture profiles during rice drying and the final equilibration using MRI with the CTI sequence.

3.3. Mathematical modeling and parameter estimation

Parameter estimation of drying models from MRI data has already been developed in other materials like concrete, gelatin, pasta or apple tissue using the Boltzmann transformation procedure [6,7], but such an approach is restricted to a semi-infinite slab geometry. Verstreken et al. [9] studied the model prediction of NMR data and showed that a statistical approach to deal with error associated to the NMR measure is necessary. In order to model the rice drying process the following hypothesis were formulated:

1. The paddy rice grain is considered as a homogeneous and isotropic medium.
2. Rice drying is a purely diffusive process where the main driving force is the liquid moisture gradient.

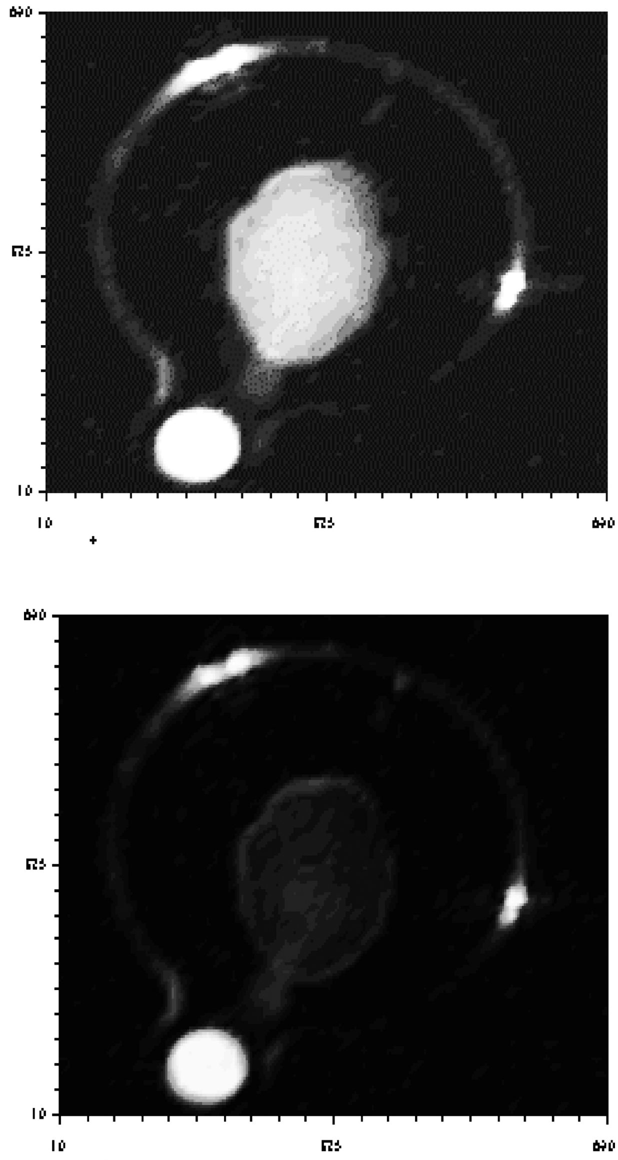

Fig. 2. MRI images of the selected region of interest in the rice grain. The color represents the intensity of the NMR signal.

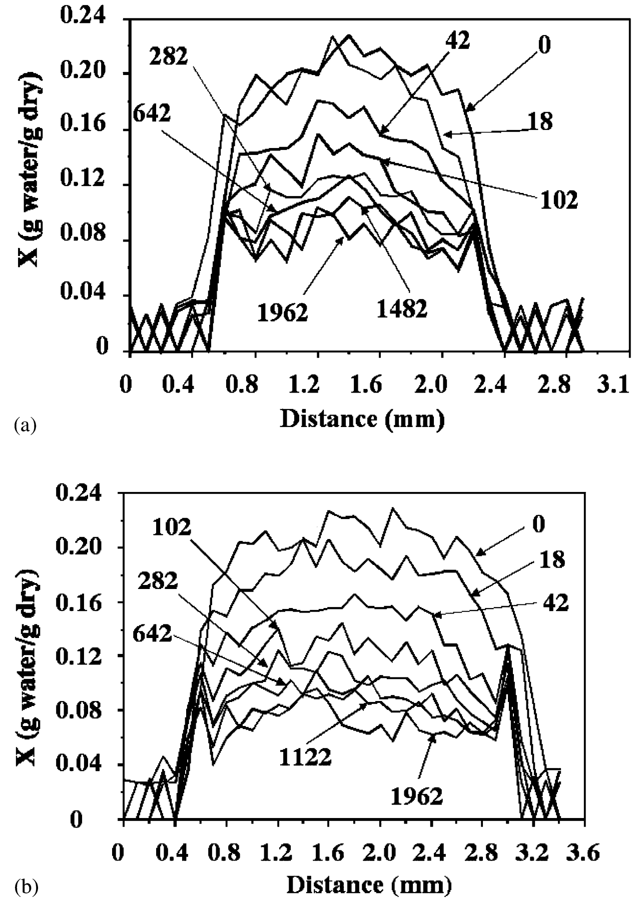

Fig. 3. Evolution during drying of moisture profile data extracted from the short (A) and long axis (B) of a rice grain at 30 °C. Lines and labels indicate the drying times in minutes.

3. Shrinkage of the rice, which occurs due to the water loss, is mainly found in the radial direction r and modeled using a solid-based coordinate system defined in ξ.
4. The temperature T of the rice grain is considered uniform all over the paddy rice grain.
5. Water transport occurs mainly in the radial direction. The transport along each of the axes is modeled as a diffusive transport in an equivalent infinite cylinder of the same dimension.

Under those assumptions the model equations that govern the drying and shrinkage of an infinite shrinking cylinder are:

Mass transfer:

$$\frac{\partial X}{\partial t} = \frac{1}{\xi}\frac{\partial}{\partial \xi}\left(\mathcal{D}_\xi \xi \frac{\partial X}{\partial \xi}\right) \tag{4}$$

where

$$\mathcal{D}_\xi = \mathcal{D}_{\text{eff}}(X, T)\left(\frac{\partial \xi}{\partial r}\right)^2 \tag{5}$$

with

$$\left.\frac{\xi\, \mathrm{d}\xi}{r\, \mathrm{d}r}\right|_t = \frac{1}{1+\beta X} \tag{6}$$

where β is the volumetric shrinkage coefficient. Considering hypothesis 3

$$\frac{\rho_s^*}{\rho_s} \approx \left(\frac{r^*}{r}\right) = \frac{1}{1+\beta(X-X^*)} \tag{7}$$

An exponential function of the moisture content and an Arrhenius type function of the temperature were used to model the effective diffusivity dependence on the moisture and temperature [17]:

$$\mathcal{D}_\xi = \mathcal{D}_{\text{ref}}\, \mathrm{e}^{aX}\, \mathrm{e}^{-E_a/R(1/T+273-1/T_{\text{ref}})}\left[\frac{1}{1+\beta X}\left(\frac{r}{\xi}\right)\right]^2 \tag{8}$$

A reference temperature of 45 °C was chosen.

Initial and boundary conditions:

i.c. : $t = 0 \quad \forall 0 < \xi < \xi_m \Rightarrow X = X_0$

b.c.1: $t > 0, \quad \xi = 0 \Rightarrow \left(\frac{\partial X}{\partial \xi}\right)_{\xi=0} = 0$

b.c.2: $t > 0,$

$$\xi = \xi_m \Rightarrow \left(\frac{\partial X}{\partial \xi}\right) = -\left(\frac{k_p S_v}{\rho_s^* \mathcal{D}_{eff}}\right)(p_{v_{air}} - p_{v_{prod}})$$

Heat transfer:

The thermal balance to a uniform temperature body is [18].

$$\frac{dT}{dt} = \frac{s_v \lambda_m k_p}{\rho_s^*(c_{p_s} + c_{p_w}\bar{X})}[65(T_{db} - T) + (P_{v_{air}} - P_{v_{prod}})] \tag{9}$$

Initial conditions:

i.c. : $t = 0 \quad \Rightarrow \quad T = T_0$

The radius at each ξ position at any time can be calculated by

$$r = \left(\int_0^{\xi} (1 + \beta X)\xi \, d\xi\right)^{1/2} \tag{10}$$

Finally, the average moisture content can be determined by

$$\bar{X} = \int_0^{R^2} \frac{X}{R^2} \, dr^2 \tag{11}$$

Physical properties of the Ariete rice and the desorption isotherm from [19] were used, and the model was simulated using the numerical methods described in [20].

Uni-dimensional moisture profiles from the MRI images were extracted from axis at 0°, 45°, 90° and 135° from the center of the rice grain. A weighted least squares procedure was posed between the experimental data and the simulated one. The objective function was the residual between the predicted and experimental moisture content inside the rice kernel. Zero weights were given to the pixels that fell out of the shrinking rice boundaries.

The unknown model parameters to be estimated were $\mathcal{D}_{ref}$, a, E_a and k_p. It was necessary to add a fifth parameter (HRF) in order to correct a systematic over-prediction of moisture content at the surface of the kernel. The possible interpretation of this is due to the fact that sorption isotherms are measured on whole kernels equilibrated at different a_w and then linked to the averaged moisture content of the kernel. However, the moisture content of the rice kernel surface is certainly lower due to the presence of lipids in the aleurone layer. In this way HRF is a multiplying factor of the moisture content in the desorption isotherm that can correct this effect.

The least squares procedure involved over 7392 points without zero weight and it was repeated with different starting values until convergence occurred. The parameters and their respective associated errors (using the classical linear approximation) are presented in Table 1.

Table 1
Parameter estimation results

Parameter	Value	95% Low	95% High
$\mathcal{D}_{ref}$	3.68×10^{-13}	3.60×10^{-13}	3.76×10^{-13}
a	8.3×10^{-2}	2.9×10^{-2}	13.7×10^{-2}
E_a	2.43×10^{1}	2.42×10^{1}	2.44×10^{1}
k_p	5.53×10^{-7}	5.41×10^{-7}	5.67×10^{-7}
HRF	1.490	1.488	1.492
$\sum(X_i - X_p)^2$	4.427		
R^2_{adj}	0.97		
σ_{res}	2.448×10^{-2}		

An example of the model fit is showed on Fig. 4. The prediction can be considered reasonable, but some limitations must be taken into account: the simplification of the kernel geometry and the fact that the presence of lipids in the surface layer can greatly influence the moisture flux, aspect that cannot be considered by a purely isotropic diffusive.

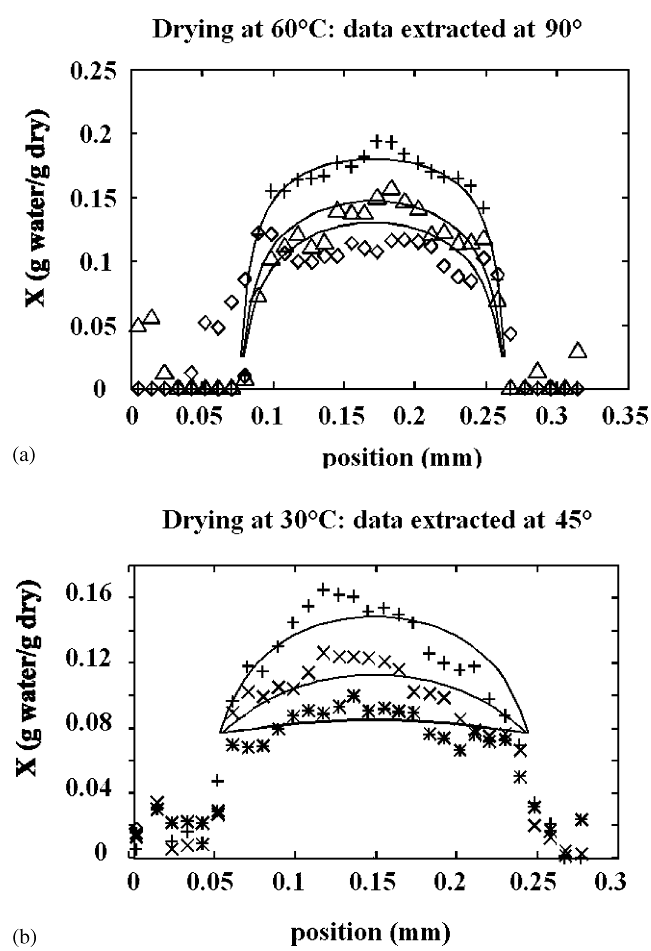

Fig. 4. Prediction of the model on two different axis (90° and 45°) for a drying experiment at 30 °C and 60 °C, respectively. Lines correspond to model prediction to compare with experimental data (symbols).

One of the most important assumptions of the presented model is the consideration of the importance of taking shrinkage into account during the drying of the grain. In fact, if considering only the final geometry of the rice grain, shrinkage does not have a very big effect on it (about 5% reduction in the radial direction). But there is more and more evidence that diffusion of water in starch systems follows a case II type of diffusion where the shrinking/swelling of the starchy matrix accompanying the water flux influences the diffusivity [21]. The fact of neglecting shrinkage in the parameter estimation ($\beta = 0$) led to a higher sum of squares when performing again the same parameter estimation ($SSQ_{\beta=0} = 4.81$ instead of 4.69 in the previous case); this can somehow support the hypothesis that the consideration of shrinkage in rice drying is essential in order to understand the water transport phenomena during drying.

4. Conclusions

A new technique, which followed the local moisture content during the drying of paddy rice kernels, was presented. A resolution of 0.1 mm at low moisture levels was achieved. The presence of an annular zone containing lipids, that could influence the moisture transport close to the surface of grain, was stated. The experimental setup provided the possibility of modeling the moisture transport phenomena and estimating the parameters of a diffusive model from the NMR data collected during drying. The model was able to simulate the evolution of the moisture profiles during the drying kinetics and stated the importance of shrinkage in the consideration of the water transport during paddy rice drying.

Acknowledgements

The present research work was made under the scope of the Quality In Drying (QUID Project, contract no. FMRX-CT96-0082) European research project. The authors would like to acknowledge the helpful discussions on the modeling issues with Dr. Roman Peczsalski.

References

[1] P. Bernada, S. Strenström, S. Mansson, Experimental study of the moisture distribution inside a pulp sheet using MRI. Part II. Drying experiments, J. Pulp Pap. Sci. 24 (1998) 380–387.
[2] A.J. Kovács, M. Neményi, Moisture gradient vector calculation as a new method for evaluating NMR images of corn (*Zea mays* l.) kernels during drying, Magn. Reson. Imaging 17 (1999) 1077–1082 (Technical Note).
[3] M. Fukuoka, H. Watanabe, T. Mihori, S. Shimada, Moisture diffusion in a dry soybean seed measured using pulsed field gradient NMR, J. Food Eng. 23 (1994) 533–541.
[4] S. Takeuchi, M. Fukuoka, Y. Gomi, M. Maeda, H. Watanabe, An application of magnetic resonance imaging to the real time measurement of the change of moisture profile in a rice grain during boiling, J. Food Eng. 33 (1997) 181–192.
[5] S. Takeuchi, M. Maeda, Y. Gomi, M. Fukuoka, H. Watanabe, The change of moisture distribution in a rice grain during boiling as observed by NMR imaging, J. Food Eng. 33 (1997) 281–297.
[6] M.J. McCarthy, E. Perez, Model for transient moisture profiles of a drying apple slab using data obtained with magnetic resonance imaging, Biotechnol. Progr. 7 (1991) 540–543.
[7] M.A. Ruiz-Cabrera, J.D. Daudin, L. Foucat, J.P. Renou, Une nouvelle methode d'estimation de la diffusivité de l'eau dans les materiaux biologiques—test sur la gélatine, in: Phenomenes de transfert, Paris 97, Récents Progrés en Génie des Procédés, Vol. 11, Nancy, France, 1997, pp. 1–6.
[8] B.P. Hills, J. Godward, K.M. Wright, Fast radial NMR microimaging studies of pasta drying, J. Food Eng. 33 (1997) 321–335.
[9] E. Verstreken, P.V. Hecke, N. Scheerlinck, J.D. Baerdemaeker, B. Nicolai, Parameter estimation for moisture transport in apples with the aid of NMR imaging, Magn. Reson. Chem. 36 (1998) 196–204.
[10] M.A. Ruiz-Cabrera, Détermination de la relation entre la diffusivité de l'eau et la teneur en eau dans les matériaux déformables à partir d'images RMN—elaboration de la méthode avec des gels de gélatine et transposition à la viande, Ph.D. Thesis, Université d'Auvergne Clermont-Ferrand, 1999 (in French).
[11] W.L.E. Spiess, W.R. Wolf, The results of the cost 90 project on water activity, in: R. Jowitt, et al. (Eds.), Physical Properties of Foods, Applied Science Publishers, London, 1983, pp. 65–87.
[12] L. Pel, H. Brocken, Determination of moisture diffusivity in porous media using moisture concentration profiles, Int. J. Heat Mass Tran. 39 (1996) 1273–1280.
[13] S.D. Beyea, B.J. Balcom, T.W. Bremner, P.J. Prado, D.P. Green, R.L. Armstrong, P.E. Grattan-Bellew, Magnetic resonance imaging and moisture content profiles of drying concrete, Cement Concrete Res. 28 (1998) 452–463.
[14] A.C. Hindmarsh, Odepack: a systematized collection of ode solvers, in: Scientific Computing, R.S. Stepleman et al. (ed.), Vol. 1, IMACS Trans. Sci. Comput., Amsterdam, 1983, pp. 55–64.
[15] P.R.T. Boggs, R.H. Byrd, J.R. Donaldson, R.B. Schanbel, Algorithm 676-ODRPACK: software for weighted orthogonal distance regression, ACM Trans. Math. Software 15 (1989) 348–364.
[16] S. Gravina, D. Cory, Sensitivity and resolution of constant-time imaging, J. Magn. Reson. Ser. B 104 (1994) 53–61.
[17] R. Peczalski, P. Laurent, J. Andrieu, J. Boyer, M. Boivin, Drying induced stress build-up within spagetti, in: A. Mujumdar (Ed.), Drying'96—Proceedings of the 10th International Drying Symposium, Vol. B, Krakóv, Poland, 1996, pp. 895–816.
[18] C.O. Rovedo, C. Suarez, P.E. Viollaz, Drying simulation of a solid slab with three-dimensional shrinkage, Dry. Technol. 13 (1995) 371–393.
[19] M. Abud Archila, Modélisation simultanée des transferts et de l'evolution de la qualité technologique du riz paddy en vue d'optimiser les conditions de séchage, Ph.D. Thesis, ENSIA, Massy, 2000 (in French).
[20] R.F. Sincovec, N.K. Madsen, Software for nonlinear partial differential equations, ACM Trans. Math. Software 1 (1975) 232–260.
[21] I. Hopkinson, R.A.L. Jones, S. Black, D.M. Lane, P.J. McDonald, Fickian and case II diffusion of water into amylose: a stray field NMR study, Carbohyd. Polym. 34 (1997) 39–47.